INTERNATIONAL SOCIETY FOR SOIL MECHANICS AND GEOTECHNICAL ENGINEERING

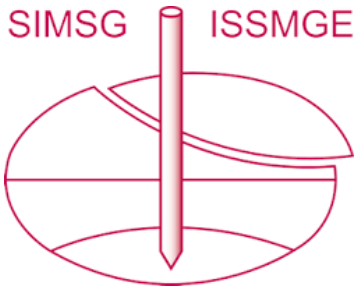

This paper was downloaded from the Online Library of the International Society for Soil Mechanics and Geotechnical Engineering (ISSMGE). The library is available here:

https://www.issmge.org/publications/online-library

This is an open-access database that archives thousands of papers published under the Auspices of the ISSMGE and maintained by the Innovation and Development Committee of ISSMGE.

The paper was published in the Proceedings of the 8th International Symposium on Deformation Characteristics of Geomaterials (IS-PORTO 2023) and was edited by António Viana da Fonseca and Cristiana Ferreira. The symposium was held from the 3rd to the 6th of September 2023 in Porto, Portugal.

IS-PORTO 2023 PROCEEDINGS

Proceedings of the 8th International Symposium on DEFORMATION CHARACTERISTICS OF GEOMATERIALS Porto, 3rd - 6th September 2023

Determination of hypoplastic parameters for a typical gravel backfill material of railway bridges

Alexander Stastny[1,2#], *Lukas* Knittel[3,4], *Thomas* Meier[5] and *Franz* Tschuchnigg[1]

[1] *Graz University of Technology, Institute of Soil Mechanics, Foundation Engineering and Computational Geotechnics, Rechbauerstraße 12, 8010 Graz (Austria),* [2] *DB Netz AG, Richelstraße 3, 80634 München (Germany),*
[3] *Keller Grundbau GmbH, Schwarzwaldstraße 1, 77871 Renchen,* [4] *former: Karlsruhe Institute of Technology (KIT), Institute of Soil Mechanics and Rock Mechanics, Engler-Bunte-Ring 14, 76131 Karlsruhe*
[5] *Baugrund Dresden Ingenieurgesellschaft mbH, Kleiststraße 10a, 01129 Dresden*
[#]*Corresponding author: alexander.stastny@deutschebahn.com*

ABSTRACT

Laboratory test programs on gravel are rare due to the maximum grain size of the material. In this paper an experimental program with triaxial tests under cyclic loading and oedometric tests on highly compacted gravel specimens, representative for bridge backfills materials, is summarized. It is used to calibrate a hypoplastic constitutive model, which includes an extension for intergranular strain to account for the cyclic loading behaviour. So far calibrated parameter sets of this soil model are scarce in literature, especially for coarse grained materials. The calibrated parameter set can be used in numerical studies, e. g. on the cyclic soil structure interaction of integral railway bridges.

Keywords: cyclic loading, triaxial tests, gravel material, hypoplasticity with intergranular strain

1. Introduction

Granular backfills of railway bridges in Germany are typically designed with compacted layers of well-graded sand and gravel materials (DB Netz AG 2021). Behind integral bridge abutments (Fig. 1a) these coarse-grained backfills are exposed to seasonal cyclic loadings due to the temperature deformation of the bridge superstructure as illustrated in Fig. 1b. This can lead to ratcheting effects, e. i. increasing earth pressures during the summer periods and settlement accumulation in the winter periods. To reproduce this behaviour in numerical analyses, powerful constitutive models are required, that can capture the cyclic loading effects and the connected densification in the soil. The well-known hypoplastic constitutive model by von Wolffersdorff (1996) with intergranular strain extension by Niemunis and Herle (1997) – short Hypo+IGS – is a promising candidate in this endeavour. Its state depends on the soil´s relative density and hence it is able to simulate densification during cyclic loading.

Up to this point only few calibrated hypoplastic parameter sets for gravel materials have been published (Herle and Gudehus 1999, Herle 2000, Schünemann 2006, Rondón et al. 2007). However, these parameter sets have mainly been derived with a focus on monotonic loading, e. i. the hypoplastic model without IGS extension, and often do not include small strain measurements. Therefore, a rather comprehensive testing program has been conducted on a typical gravel backfill material at the Karlsruhe Institute of Technology (Stutz et al. 2022), which will be presented in the following. Most of the tested specimens were highly compacted to represent in situ conditions. The test series includes oedometric compression tests with multiple un- and reloading stages as well as monotonic and cyclic triaxial tests in drained and undrained conditions. Furthermore, small strain measurements have been performed during drained cyclic triaxial tests using Bender-Elements and local deformation transducers. Based on the test data, first calibration results of the Hypo+IGS model will be shown in this paper.

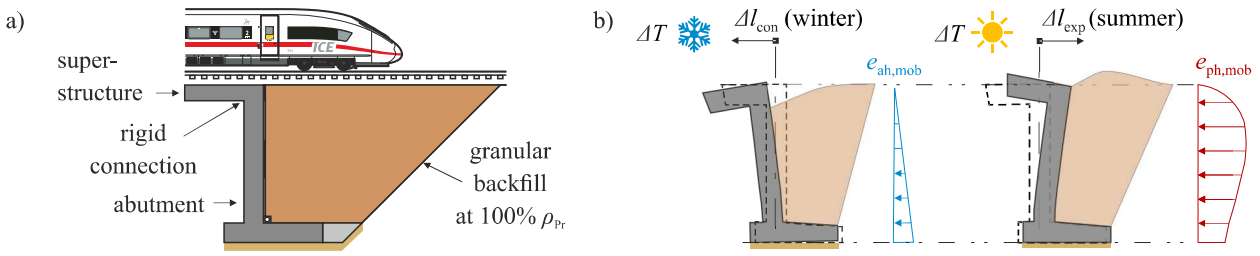

Figure 1. a) Integral railway bridge with a rigid connection of superstructure and the abutment b) cyclic soil-structure interaction mechanism of an integral abutment and its granular backfill due to seasonal temperature loading

2. Hypoplastic model

Von Wolffersdorff (1996) postulated a hypoplastic soil model, which incorporates soil nonlinearity as well as stress- (barotropy) and density-dependency (pyknotropy). It has a rate dependent formulation and thus does not distinguish between elastic and plastic strains. Although the model performs well for the simulation of monotonic loading in non-cohesive soils, it is not suitable for cyclic loading and shows a severe ratcheting behaviour (Niemunis and Herle 1997). Therefore, an extension of this model was proposed by Niemunis and Herle (1997) to improve the small strain and cyclic loading behaviour of the model. The intergranular strain tensor $\mathbf{h}$ (IGS) was introduced, that memorizes the most recent strain history and increases the stiffness after a strong strain reversal. The Hypo+IGS model can be expressed in a single tensorial equation that connects the strain rate $\dot{\boldsymbol{\varepsilon}}$ with the effective stress rate $\dot{\boldsymbol{\sigma}}$ (both second order tensors):

$$\dot{\boldsymbol{\sigma}} = \mathbf{M}(\boldsymbol{\sigma},\mathbf{h},e) : \dot{\boldsymbol{\varepsilon}} \tag{1}$$

Its fourth order stiffness tensor $\mathbf{M}$ is a function of the three state variables (effective stress $\boldsymbol{\sigma}$, the intergranular strain $\mathbf{h}$ and the void ratio e) and can be expressed as:

$$\mathbf{M} = [\rho^{\chi} m_T + (1-\rho^{\chi}) m_R]\,\mathbf{L} + \begin{cases} \rho^{\chi}(1-m_T)\mathbf{L} : \vec{\mathbf{h}}\,\vec{\mathbf{h}} + \rho^{\chi}\,\mathbf{N}\,\vec{\mathbf{h}} & \text{for } \vec{\mathbf{h}} : \dot{\boldsymbol{\varepsilon}} > 0 \\ \rho^{\chi}(m_R - m_T)\mathbf{L} : \vec{\mathbf{h}}\,\vec{\mathbf{h}} & \text{for } \vec{\mathbf{h}} : \dot{\boldsymbol{\varepsilon}} \le 0 \end{cases} \tag{2}$$

Here $\mathbf{L}$ (fourth order tensors) and $\mathbf{N}$ (second order) are linear respectively non-linear stiffness functions of $\boldsymbol{\sigma}$ and e. $\vec{\mathbf{h}} = \mathbf{h} / \|\mathbf{h}\|$ describes the IGS direction and $\rho = \|\mathbf{h}\| / R$ describes the current mobilization of the IGS in reference to its maximum value R. At large monotonic strains the IGS is fully mobilized with $\|\mathbf{h}\| = R$, while for cyclic loading $\|\mathbf{h}\| < R$. The material parameters m_T and m_R are multiplier, that increase the stiffness for transversal ($\vec{\mathbf{h}} : \dot{\boldsymbol{\varepsilon}} = 0$) or reversal ($\vec{\mathbf{h}} : \dot{\boldsymbol{\varepsilon}} = -1$) strain loading. For large monotonic strains the tangent stiffness $\mathbf{M}$, i. e. the response of the extended Hypo+IGS model, matches the stiffness of the basic hypoplastic model.

Table 1. Summary of the Hypo+IGS material parameter

Parameter		Description
φ_c	[°]	Critical state friction angle
e_{d0}	[-]	Min. void ratio at effective mean stress p = 0 kPa
e_{c0}	[-]	Critical void ratio at p = 0 kPa
e_{i0}	[-]	Max. void ratio at p = 0 kPa
h_S	[GPa]	Granular hardness – controls the overall slope of compression curves
n	[-]	Power stiffness exponent – controls curvature of compression curves
α	[-]	Dilatancy exponent – controls the peak friction angle and hence the dilatancy
β	[-]	Pyknotropy exponent – influences the size of the response envelope (both bulk and shear stiffness)
m_R	[-]	Stiffness factor for reversal loading
m_T	[-]	Stiffness factor for transversal loading
R	[-]	Elastic strain amplitude
β_r	[-]	Parameter controlling stiffness decay
χ	[-]	Parameter controlling stiffness decay

As input eight hypoplastic (φ_c, h_s, n, e_{c0}, e_{d0}, e_{i0}, α, β) plus five additional IGS parameters (R, m_R, m_T, β_r, χ) are required. They are briefly summarized in Table 1. The full mathematical description as well as further details of the soil models can be found in von Wolffersdorff (1996) and Niemunis and Herle (1997).

Guidance on the calibration of the Hypo+IGS model is given in Herle (1997), Herle and Gudehus (1999), Rondón et al. (2007), Meier (2008), Wegener and Herle (2014) and Mašín (2019). These recommendations will be applied in the following chapters.

3. Test series on gravel material

The main purpose of bridge backfills is to permanently withstand dead or traffic loads of any kind with as little elastic and plastic deformation as possible while allowing a proper drainage of the traffic way and enclosed dams. Coarse grained, well-graded materials are best suited for this task, as the Proctor density and therefore the compactability of the soil strongly increases with higher uniformity of the grain size distribution (Lauer 2021). In Germany only sands and gravels with less than 5% fine grains ≤ 0.063 mm (DIN EN ISO 14688-1) and a uniformity coefficient $C_u \geq 6$ can be used for granular backfill designs. Also, a compaction to 100% of Proctor density ρ_{Pr} in layer of 30 cm is mandatory (DB Netz AG 2021).

In this experimental program a well graded subrounded gravel material (Fig. 3) with a uniformity coefficient $C_u = 24$, a mean grain size of $d_{50} = 4$ mm and a maximum grain size of $d_{100} = 16$ mm was tested. Due to its properties, it represents a typical backfill gravel. Its grain density is $\rho_s = 2.636$ g/cm³ and with index tests (DIN 18126) a maximum and minimum void ratio of $e_{max} = 0.442$ and $e_{min} = 0.271$ were determined. Proctor tests with modified energy gave a dry Proctor density of $\rho_{Pr} = 2.05$ g/cm³ at $w_{Pr} = 8\%$, which corresponds to a relative density index of $I_{D,Pr} = 0.918$ at a void ratio of $e_{Pr} = 0.286$. The testing program consists of several components:

a) Preliminary tests for classification and density determination
b) Pluviated cone tests for the determination of the angle of repose (critical state friction angle φ_c) at loose conditions
c) 3x oedometric compression tests (OED) with several un- and reloadings for the calibration of stiffness parameters
d) 3x monotonic triaxial tests with drained conditions (DMT) at different initial mean stresses p_0 for the determination of shear stiffness and dilatancy parameters
e) 2x cyclic triaxial tests with undrained conditions (UCT) at N = 79 and 100 cycles to calibrate cyclic parameters
f) 3x cyclic triaxial tests (Fig 2) with drained conditions (DCT) on prismatic specimens with Bender-Elements (BE) as well as local strain measurements (with local deformation transducer LDT) to determine the small strain and cyclic parameters. In these tests increasing cyclic shear stress amplitudes q^{ampl} were applied with two cycles N at each

stress amplitude. In Knittel (2020) and Knittel et al. (2020) a detailed description of the triaxial apparatus and the procedure for the small strain measurement is given.

The oedometric and triaxial test conditions are given in Table 2. A specimen-to-grain size ratio of $d / d_{100} = 6.25$ for cylindrical specimens (DMT, UCT) and $b / d_{100} = 5.4$ for specimens with square cross section of $A = b \cdot b = 76$ cm² (DCT) was reached. The majority of specimens were prepared in the range of the modified Proctor density to represent the in situ compaction. The triaxial samples were compacted in five layers by dry tamping, while the larger oedometric specimens were prepared by dry air pluviation and densified by vibration on a shaking table. More details on the test program will be presented in an upcoming publication.

Table 2. Summary of the triaxial and oedometric tests

Test series	Specimen size	I_{D0} [-]	p_0 [kPa]	q^{ampl} [kPa]	N [-]
OED	h = 16 cm, d = 50 cm	0.07 0.91 0.93	-	-	-
DMT	h = 10 cm, d = 10 cm	0.95 0.95 0.98	50 100 300	-	-
UCT	h = 10 cm, d = 10 cm	0.84 0.87	50 100	25 25	79 100
DCT with BE- and LDT-measurement	h = 18.3 cm, A = 76 cm²	0.87 0.86 0.79	50 100 300	5 –150	9x2 4x2 8x2

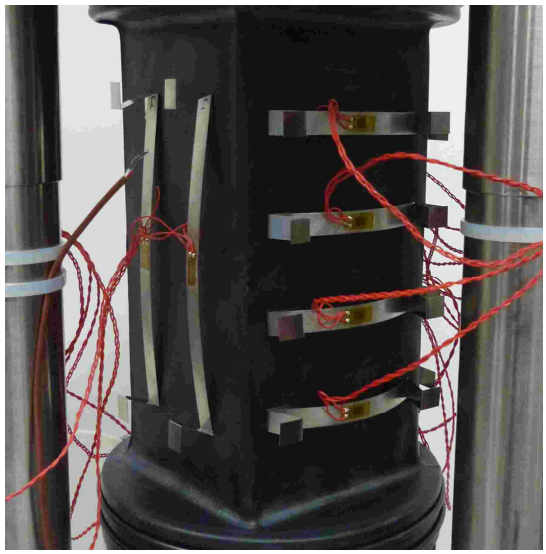

Figure 2. Dry prismatic specimen in black rubber membrane placed in the triaxial apparatus (without cell) with Bender-Elements at both end plates and LDTs for local strain measurements applied horizontally and vertically on the sample sides

4. Calibration of the soil model parameter

The calibration of the Hypo+IGS model based on the experimental results requires several steps, which will be shown back-to-back in the following. Any supporting element test simulation in this study was conducted with the Incremental Driver (ID) software by Niemunis (2017) and the Hypo+IGS UMAT by Mašín et al. (2017).

First of all, the eight hypoplastic parameters were determined according to Herle and Gudehus (1999), Meier (2008) and Mašín (2019). *[Step 1]* From the inclination of five pluviated cone tests a critical friction angle of $\varphi_c = 34.4°$ for (very) loose conditions (see Fig. 3) was derived with a small scatter of ±0.6°, following the recommendation in the three literature sources mentioned above. The results for φ_c from DMT tests are not considered as these tests were performed on very dense specimens which additionally showed shear band localization at large strains.

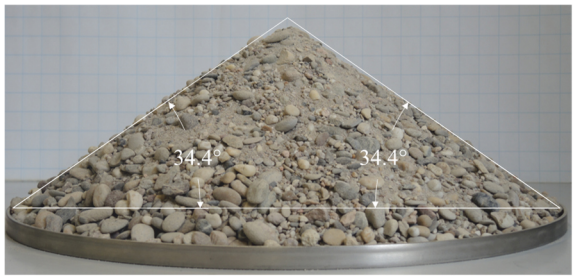

Figure 3. Pluviated cone of the test material with the average measurement for the critical friction angle φ_c

[Step 2] The parameters for the minimum void ratio e_{d0} at $p = 0$ and the critical state void ratio e_{c0} at $p = 0$ were estimated from $e_{d0} \approx e_{min} = 0.271$, $e_{c0} \approx e_{max} = 0.442$. For the subrounded gravel in this investigation the parameter for the maximum void ratio e_{i0} at $p = 0$ was determined from $e_{i0} = 1.1 e_{max} = 0.486$, analog to the ratio $e_{i0} / e_{max} = 0{,}9$ in Herle (1997) for subrounded Hochstetten gravel.

[Step 3] Following the procedure in Herle and Gudehus (1999) and Mašín (2019) the stiffness parameter $h_s = 1.8$ MPa and $n = 0.26$ were estimated by fitting Eq. (3) on the results of the oedometric compression test (OED) with a dry, very loose specimen ($I_{D0} = 0.068$):

$$\frac{e_i}{e_{i0}} = \frac{e_c}{e_{c0}} = \frac{e_d}{e_{d0}} = \exp\left[-\left(\frac{3p}{h_s}\right)^n\right] \tag{3}$$

using $p = (\sigma_1 + 2\sigma_3)/3$ and $\sigma_3 = K_0\,\sigma_1$ with effective mean stress σ_1 and σ_3 and $K_0 = 1 - \sin\varphi_c$. In a consecutive step the initial loading path of the OED test was simulated with Incremental Driver. To improve the reproduction of the test results in Fig. 8c both parameters were slightly changed to $h_s = 2$ MPa and $n = 0.25$.

[Step 4] At next back calculations of the drained triaxial tests (DMT) at initial mean pressures of $p_0 = 50$, 100 and 300 kPa (see Fig. 4) were conducted to calibrate the stiffness parameter β and the dilatancy parameter α. As suggested in Meier (2008) and Mašín (2019), α is used to control the peak deviatoric stress q (Fig. 4a) and the dilatancy behaviour (Fig. 4b), while β is adjusted to influence the initial stiffness and the peak location in Fig. 4a. For $\alpha = 0.22$ and $\beta = 3$ a good agreement of simulation and experimental data was reached based on engineering judgement. This calibration result for the parameter α and β (and h_s, n) should be regarded as preliminary. The final parameter set will be found by an iterative calibration of these (and the IGS) parameters to reach the best possible reproduction of all element tests from Table 2. Before that the five IGS parameters were calibrated in *step 5 + 6*.

[Step 5] Based on the results of the three cyclic triaxial tests (DCT) with local strain measurements, fitting curves were derived from Oztoprak and Bolton (2013) for the shear stiffness degradation (G/G_0) with increasing shear strain amplitude γ^{ampl}. The results are illustrated in Fig. 5. The constant R, which represents the elastic strain amplitude in the IGS formulation can be estimated from these curves as the shear strain $\gamma_{0.8} \approx R$ at $G/G_0 = 0.8$ (Wegener and Herle 2014). Similar to recommendations in literature (Meier 2008 and Mašín 2019) for coarse grained soils, a value of $R \approx 1 \cdot 10^{-4}$ was found. Additionally, the maximum shear modulus G_0 can be read from the fitting curves at very small shear strain amplitudes $\gamma^{ampl} = 1 \cdot 10^{-6}$. A comparison of these LDT readings to the Bender-Element (BE) measurements at the beginning of every DCT test is shown in Fig. 6. Although the results for G_0 from LDT and BE measurements differ in part, they still are a good calibration basis for the IGS small strain stiffness parameter m_R. From the back-calculation of four DCT tests with very small strain amplitudes $\Delta\gamma^{ampl} \leq 1 \cdot 10^{-6}$ at $p_0 = 50$, 100, 200 and 300 kPa a good reproduction of the $G_0 - p_0$ curves (shown in Fig. 6) was achieved for $m_R = 5.2$. For the IGS small strain stiffness parameter for transversal loading m_T no experiment has been conducted. Its value was estimated based on the recommendation in Mašín (2019): $m_T = 0.7$, $m_R = 3.6$.

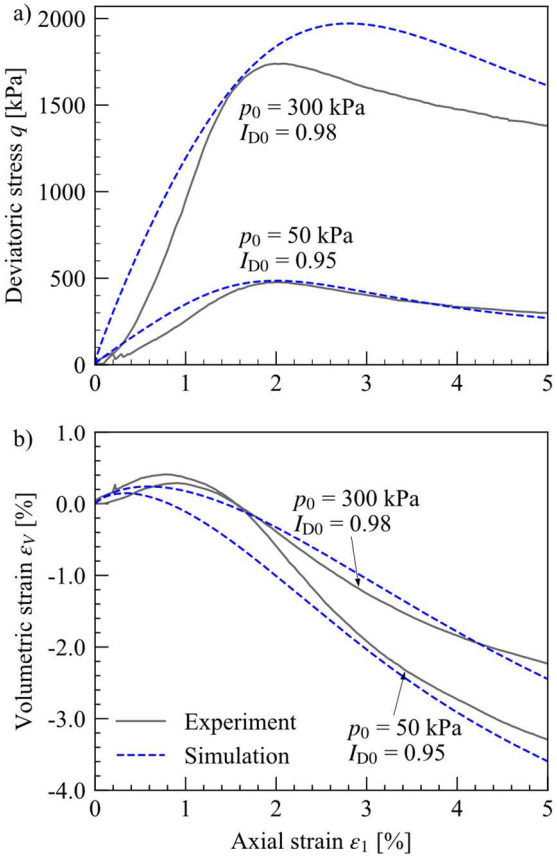

Figure 4. Experimental results (solid lines) and simulations (dashed lines; final parameter set) of DMT tests on highly compacted samples ($I_{D0} \approx 0.95 - 0.98$) at initial mean pressures $p_0 = 50$ and 300 kPa

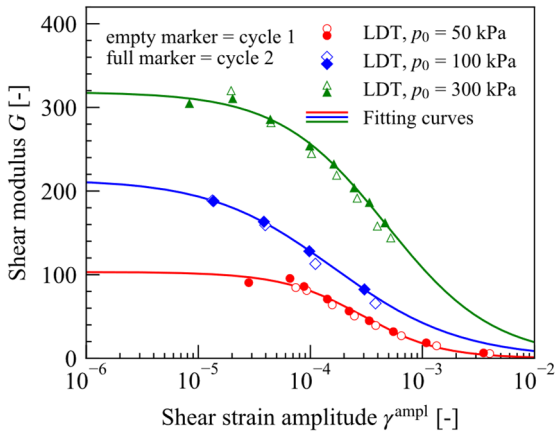

Figure 5. Degradation of the shear modulus G with increasing shear strain γ^{ampl} from LDT measurements in DCT tests with increasing cyclic shear stress amplitudes

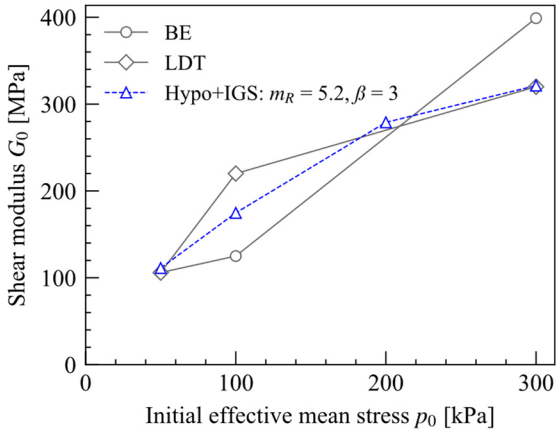

Figure 6. Calibration of parameter m_R based on BE and LDT measurements of G_0

[Step 6] The last two IGS parameter β_r and χ were calibrated by re-calculations of the cyclic triaxial tests (UCT) in undrained conditions listed in Table 2, as suggested in Mašín (2019). Fig. 7a shows the evolution of p while Fig. 7b shows the evolution of the pore water pressure $\Delta u^{acc}(N)/p_0$ along cycles. The best fit of these curves was achieved for $\beta_r = 0.1$ and $\chi = 1.3$.

[Step 7] In the final calibration step the Hypo+IGS parameters are iteratively optimized to reach an equally good reproduction of OED, DMT, DCT and UCT element tests. At first the OED tests on the very dense specimens ($I_{D0} = 0.913$, 0.931) in Fig. 8a and 8b are simulated. The parameter $\beta = 2.5$ and $\chi = 1.2$ were slightly adjusted to match the softer test behaviour. A further reduction of β and / or m_R (together with an adaptation of χ and β_r) would reproduce these very dense oedometric compression tests even better. Yet, this would significantly worsen the simulation of the triaxial tests DMT in Fig. 4 (in case of a reduced β value) and DCT in Fig. 6.

Subsequently, the DMT and UCT tests were re-calculated. Here only $\alpha = 0.23$ had to be slightly corrected, which indicates that no further iteration is necessary. Thus, the final parameter set was found, which is summarized in Table 3.

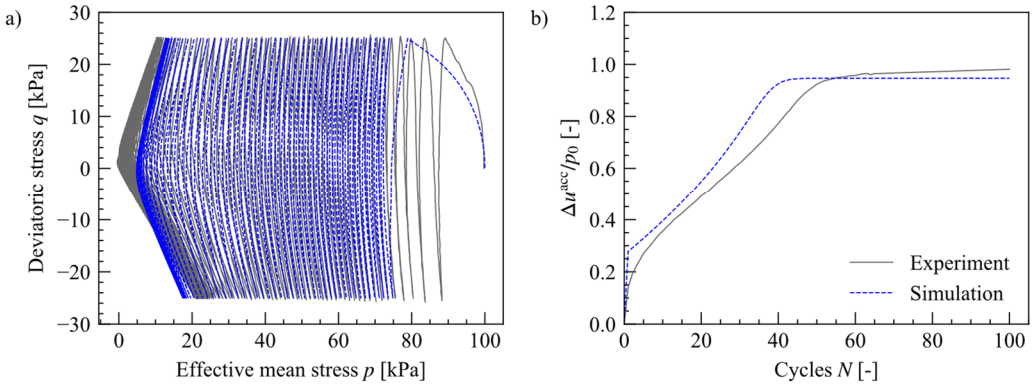

Figure 7. Experimental results (solid line) and simulation (dashed line, final parameter set) of a UCT test on a highly compacted specimen (I_{D0} = 0.87) with isotropic consolidation of p_0 = 100 kPa and 100 stress-controlled cycles at q^{ampl} = ±25 kPa

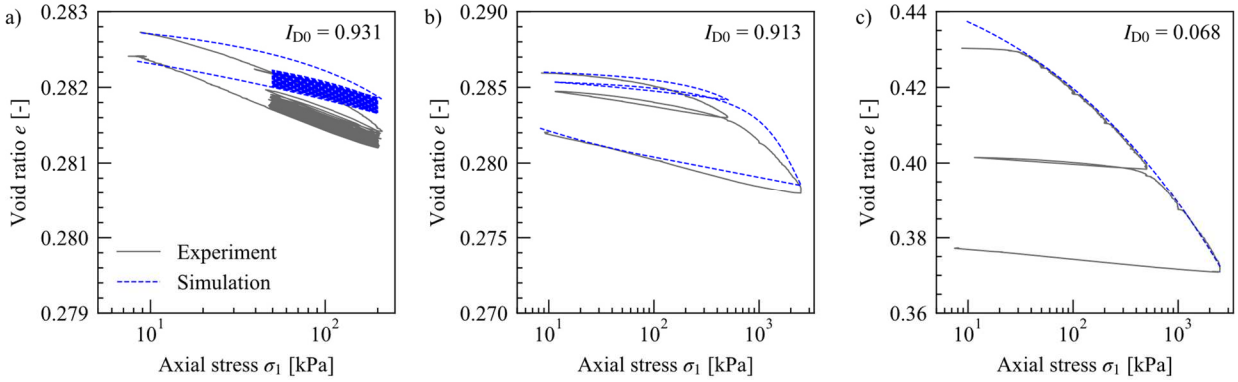

Figure 8. Experimental results (solid lines) and simulations (dashed lines; final parameter set) of OED tests with un- and reloading on highly compacted (a, b) and very loose (c) specimens

Table 3. Final Hypo+IGS parameter set for the backfill gravel

	φ_c [°]	e_{d0} [-]	e_{c0} [-]	e_{i0} [-]	h_s [GPa]	n [-]	α [-]	β [-]	m_R [-]	m_T [-]	R [-]	β_r [-]	χ [-]
Final parameter set	34.4	0.271	0.442	0.486	2	0.25	0.23	2.5	5.2	3.6	$1 \cdot 10^{-4}$	0.1	1.2

5. Conclusion

A series of monotonic and cyclic element tests has been conducted on a typical gravel backfill material for railway bridges. The experimental program comprehends oedometric compression tests as well as monotonic and cyclic triaxial tests in drained and undrained conditions. Furthermore, small strain measurements were performed by means of local deformation transducer (LDTs) and Bender-Elements (BE) in drained cyclic triaxial tests. To account for the in situ conditions, the majority of tests were performed on dense to very dense specimens in the range of the Proctor density.

In this paper the extensive program serves as a thorough calibration base for the Hypo+IGS soil model with focus on cyclic loading. To the author´s knowledge such parameter sets are rarely available in literature, especially with focus on the small strain and cyclic IGS parameter. The calibration steps and first calibration results are briefly described. More details on the experimental program, the parameter calibration and the performance of this and other promising soil models for cyclic loading will be discussed in upcoming publications. The calibrated soil models are used in an ongoing research project for FE-studies on the cyclic interaction of integral (railway) bridges and their granular backfill materials.

Acknowledgements

The experimental program was initiated and funded by DB Netz AG. It was conducted at the Karlsruhe Institute of Technology (KIT) under the supervision of H. Stutz, L. Knittel, H. Reith and A. Wappler and executed by the technicians H. Borowski, P. Gölz and N. Demiral.

References

DB Netz AG 2021. “Richtlinie 836: Erdbauwerke und sonstige geotechnische Bauwerke planen, bauen und instand halten”, Standard for railway earthwork construction (in German), DB Netz AG, Frankfurt am Main.

DIN 18126 2022. “Baugrund, Untersuchung von Bodenproben-Bestimmung der Dichte nicht bindiger Böden bei lockerster und dichtester Lagerung”, Standard test method for minimum and maximum densities (in German), Beuth Verlag GmbH, Berlin. http://doi.org/doi:10.31030/3329398

DIN EN ISO 14688-1 2020. “Geotechnical investigation and testing — Identification and classification of soil — Part 1: Identification and description”, Beuth Verlag GmbH, Berlin. https://dx.doi.org/10.31030/3187022

Herle, I. 1997. “Hypoplastizität und Granulometrie einfacher Korngerüste”, Hypoplasticity and granulometry of simple grain skeletons (in German). Dissertation, Karlsruhe Institute of Technology,. ISSN 0453-3267

Herle, I. 2000 “Granulometric limits of hypoplastic models”, Institute of Theoretical and Applied Mechanics, Czech AcademyTask Quarterly, Scientific Bulletin of Academic Computer Centre in Gdansk, 4(3), pp. 389–408. [online] Available at: https://bibliotekanauki.pl/articles/1954563.pdf

Herle, I., and G. Gudehus 1999. “Determination of parameters of a hypoplastic constitutive model from properties of grain assemblies”, Mechanics of Cohesive-frictional Materials, 4(5), pp. 461–486. https://doi.org/10.1002/(SICI)1099-1484(199909)4:5<461::AID-CFM71>3.0.CO;2-P

Knittel, L. “Verhalten granularer Böden unter mehrdimensionaler zyklischer Beanspruchung”. Behaviour of granular soils under multidimensional cyclic loading (in German). Dissertation, Karlsruhe Institute of Technology, 2020. ISSN: 0453-3267

Knittel, L., T. Wichtmann, A. Niemunis, G. Huber, E. Espino, and T. Triantafyllidis. 2020 “Pure elastic stiffness of sand represented by response envelopes derived from cyclic triaxial tests with local strain measurements”, Acta Geotechnica, 15 (8), pp. 2075–2088. https://doi.org/10.1007/s11440-019-00893-9

Lauer, C. 2021. “Bodenzustandsindex und zustandsabhängige Kennwerte für gemischtkörnige Böden.”, Soil state index and state dependent soil parameters for coarse-fine mixtures (in German), Dissertation, Technische Universität Dresden. ISSN: 1434-3053

Mašín, D. 2017. “Modelling of soil behaviour with hypoplasticity”, Springer series in geomechanics and geoengineering, Springer, Cham, Switzerland. ISBN: 978-3-030-03976-9

Mašín, D., P.-A. von Wolffersdorff, C. Tamagnini 2017 “Clay and Sand hypoplasticity UMAT”. [online] Available at: https://soilmodels.com/download/plaxis-umat-hypoplas-zip/

Meier, T. 2008 “Application of hypoplastic and viscohypoplastic constitutive models for geotechnical problems”, Dissertation, Karlsruhe Institute of Technology. ISSN: 0453-3267

Nagula S., and J. Grabe. 2020 .“Hypoplastic model with intergranular strain: Dependence on grain properties and initial state”, Geotechnical Engineering Journal, 51(4), pp. 122-129. ISSN 0046-5828

Ng, C., H. S. Sun, G. H. Lei, J. W. Shi, and D. Mašín 2015. “Ability of three different soil constitutive models to predict a tunnel’s response to basement excavation”, Canadian Geotechnical Journal, 52(11), pp. 1685–1698. https://doi.org/10.1139/cgj-2014-0361

Niemunis, A. 2017 “Incremental Driver, user’s manual”, Karlsruhe Institute of Technology. [online] Available at: https://www.soilmodels.com/idriver

Niemunis, A., and I. Herle. 1997 “Hypoplastic model for cohesionless soils with elastic strain range”, Mechanics of Cohesive-frictional Materials, 2(4), pp. 279–299. https://doi.org/10.1002/(SICI)1099-1484(199710)2:4<279::AID-CFM29>3.0.CO;2-8

Oztoprak, S., and M. D. Bolton. 2013. “Stiffness of sands through a laboratory test database”, Géotechnique, 63(1), pp. 54–70. https://doi.org/10.1680/geot.10.P.078

Rondón, H. A., T. Wichtmann, T. Triantafyllidis, and A. Lizcano 2007 “Hypoplastic material constants for a well-graded granular material for base and subbase layers of flexible pavements”, Acta Geotechnica, 2(2), pp. 113–126. https://doi.org/10.1007/s11440-007-0030-3

Schünemann, A. 2006. “Numerische Modelle zur Beschreibung des Langzeitverhaltens von Eisenbahnschotter unter alternierender Beanspruchung“, Numerical models for the description of the longterm behaviour of railway ballast under alternating loading (in German), Dissertation, Karlsruhe Institute of Technology. ISSN: 0453-3267

Stutz, H., H. Reith, and A. Wappler 2022. “Bericht. DB-Projekt - Laborversuche an Kies-Hinterfüllungsmaterial“, Report. DB-project - Experimental tests on gravel backfill material (in German). Tech. rep. (not published), Karlsruhe Institute of Technology.

Wegener, D., and I. Herle. 2014 “Prediction of permanent soil deformations due to cyclic shearing with a hypoplastic constitutive model”, Geotechnik, 37(2), pp. 113–122. https://doi.org/10.1002/gete.201300013

Wolffersdorff, P.-A. v. 1996. “A hypoplastic relation for granular materials with a predefined limit state surface”, Mechanics of Cohesive-frictional Materials, 1(3), pp. 251–271, https://doi.org/10.1002/(SICI)1099-1484(199607)1:3<251::AID-CFM13>3.0.CO;2-3